Journal of Materials Processing Technology 210 (2010) 1190–1196

Contents lists available at ScienceDirect

Journal of Materials Processing Technology

journal homepage: www.elsevier.com/locate/jmatprotec

Interactions between TiAl alloys and yttria refractory material in casting process

Cui Renjie*, Gao Ming, Zhang Hu, Gong Shengkai

School of Materials Science and Engineering, Beijing University of Aeronautics and Astronautics, Beijing 100191, China

ARTICLE INFO

Article history:
Received 24 November 2009
Received in revised form 28 February 2010
Accepted 2 March 2010

Keywords:
Titanium aluminides
Intermetallics
Casting
Microstructure
Thermodynamic analysis

ABSTRACT

In this work, U-shaped yttria ceramic crucibles have been prepared to melt Ti–47Al (at.%) alloy in a vacuum induction furnace, in order to simulate the worst practical situation with respect to the interactions between TiAl alloy and yttria refractory material. The effects of superheating temperature and cooling media on the metal–crucible interface, microstructure, chemical composition and microhardness have been evaluated. The investigation demonstrates that interactions between the yttria crucible and the molten TiAl consist of slight chemical dissolution and some physical erosion and the extent of the dissolution and erosion depend on the superheating temperature. The thermodynamics of TiAl–Y_2O_3 reactions have been investigated according to the calculation of the Gibbs free energy change of the yttria dissolution reaction. The possibilities of melting and casting TiAl alloys by the use of yttria refractory material are also discussed.

1. Introduction

For the last two decades, TiAl-based alloys have attracted attention as potential candidates for high-temperature structural applications in the aerospace and military. A previous study (Wang et al., 2008) showed that due to low density, high specific strength, high Young's modulus and oxidation resistance at high temperatures, these materials represent a good substitute for nickel-based superalloys. At the present stage, the production of TiAl-based alloy parts is expected to increase as a result of new emerging markets, such as automotive industry, as reported by Tetsui (2002), as well as the development of new and cheaper processing techniques than those used so far. However, Sung and Kim (2005) noted that the main factors to limit the manufacture of mass market TiAl-based components are the high reactivity of TiAl alloys with the crucible and mould at high temperatures, and the high production cost of the casting process.

In order to improve the quality of TiAl alloy castings and reduce the production cost, Kuang et al. (2000) pointed out that it is, therefore, necessary to introduce a refractory material capable of melting and casting highly reactive titanium alloys without excessive contamination. Until now, as reported by Gomes et al. (2008), no refractory material was found to be absolutely inert against TiAl alloys and some interactions between the alloy and the crucible/mould materials always occurred during melting and casting, leading to metal contamination. Taking into account the Gibbs free energy of formation, Kostov and Friedrich (2006) found that Y_2O_3 presents the most negative value among common metallic oxides, suggesting that it is a suitable material to be used as crucibles/moulds for melting and casting of TiAl alloys. Therefore, it is instructive to investigate the interaction mechanism and thermodynamic stability of yttria in contact with molten TiAl alloys.

In this paper, Ti–47Al alloys were melted in a vacuum induction melting (VIM) furnace equipped with a U-shaped yttria crucible, in order to simulate the worst practical situation with respect to the interaction between TiAl alloys and yttria refractory. The interactions were investigated by energy dispersive spectrometry (EDS), scanning electron microscopy (SEM), electron-probe microanalysis (EPMA), transmission electron microscopy (TEM), X-ray diffraction (XRD), chemical analysis and hardness tester. The aim of the present work is to examine the interactions between TiAl alloys and yttria refractory and to elucidate the interaction mechanisms. Furthermore, thermodynamic calculations of TiAl–Y_2O_3 reactions have been conducted in order to evaluate the possibilities of melting and casting TiAl alloys by the use of yttria.

2. Experimental

2.1. Melting operation

Melting testing was carried out in a vacuum induction melting furnace equipped with a U-shaped yttria crucible (Fig. 1). Melting stocks weighing 1 kg were prepared from sponge Ti and pure A1 (Table 1) in a vacuum arc melting furnace. The crucibles applied in this work were made of pure yttria powder (Table 2) using cold isostatic pressing and ordinary pressure sintering techniques. In

* Corresponding author. Tel.: +86 10 82339256.
E-mail address: rj-cui@mse.buaa.edu.cn (C. Renjie).

0924-0136/$ – see front matter © 2010 Elsevier B.V. All rights reserved.
doi:10.1016/j.jmatprotec.2010.03.003

Table 1
The chemical composition of sponge Ti and pure A1 used to produce the Ti–47A1.

Element	Chemical composition								
	Fe	Si	Cl	C	N	O	S	P	Ag
MHTi-0[a], 99.76 (wt%)	0.06	0.02	0.06	0.02	0.02	0.06	–	–	–
Al-05, 99.999% (ppm)	2.5	2.8	2.8	0.5	1.0	0.5	1.0	0.2	0.2

[a] Produced by kroll method, namely kroll method grade 0 titanium sponge.

order to control the amount of porosity to improve crucible thermal shock resistance, the yttria powder was mixed in a weight proportion of 1:1:1 with particle sizes of ≤10 μm, 10–200 μm and 200–2000 μm, respectively. The crucibles were cold isostatic pressed under 180 MPa and then sintered at 1650 °C for 10 h in a resistance heating furnace. The temperature of the furnace was raised slowly at a rate of 1 K min^{-1}. The porosity of the crucibles was 21 ± 2% measured using mercury porosimetry. The dimensions of the crucibles and graphite moulds were 115 mm o.d. × 90 mm i.d. × 120 mm inner height and 135 mm o.d. × 60 mm i.d. × 150 mm height, respectively.

Before the heating cycle, the chamber was evacuated down to ~10^{-3} bar (down to ~10^{-6} bar at the last operation) and backfilled with pure argon up to 0.05 MPa (O_2 < 10 ppm; N_2 < 50 ppm; H_2 < 5 ppm; H_2O < 15 ppm; CH_4 < 4 ppm) three times, in order to reduce the oxygen content to a minimum level and avoid the evaporation of alloy components. The superheating temperatures were 1600 °C and 1700 °C, measured and controlled by a WRe5-WRe26 thermocouple with an yttria ceramic protection sheath, corresponding to approximately 100 °C and 200 °C superheat (assuming that the liquid temperature of Ti–47A1 was 1500 °C). When the temperature reached around 1500 °C, the first liquid metal became visible. Afterwards, the thermocouple was immersed in the liquid metal to control the temperature (temperature fluctuation within a range of ±5 °C), and the induction power was controlled by an automatic temperature control system. After reaching the superheating temperature, the metal was held for 20 min in the furnace. The molten metal temperature was continuously monitored and controlled during the 20 min holding time with thermocouple. It should be noted that the yttria protection sheath was still available after several continuous temperature measurements and a slight dissolution/erosion of the protection sheath was ignored. In the first series of tests, samples were allowed to solidify and cool to room temperature inside the crucible, in order to simulate the worst practical situation. Finally, the yttria crucibles containing the solidified metal were removed from the furnace at a temperature of about 50 °C. In the second series of tests, molten metal was tilt poured into a cylindrical high purity graphite mould pre-heated to 700 °C in a resistance heating furnace before introducing it in the vacuum induction melting furnace for casting, in order to undermine the influence of oxygen and moisture pickup from the mould during the casting operation. It should be noted that the cooling rates in the yttria crucibles and graphite moulds were not measured as well as the mould temperature when the pouring operation was performed, due to the limitation of experimental conditions.

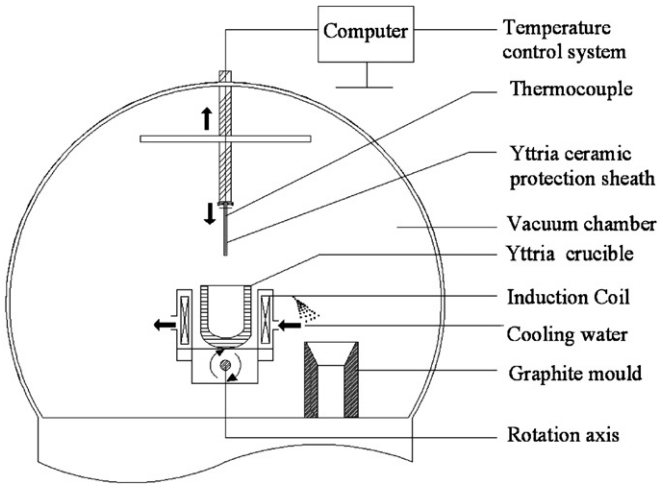

Fig. 1. Schematic diagram of the vacuum induction melting furnace equipped with a U-shaped yttria crucible.

Table 2
The chemical composition of Y_2O_3 used to produce crucible.

Element	Y_2O_3	Fe_2O_3	SiO	Al_2O_3	TiO_2
Chemical composition (wt%)	≥99.8%	≤0.02	≤0.03	≤0.02	≤0.02

2.2. Inspection of the melted samples

After melting, the obtained TiAl samples were mechanically separated from the crucible and mould materials. Samples for characterization were collected from the surface to the middle of the casting by sectioning them at 50% of their height. Electron-probe microanalysis (EPMA, JEOL JXA-8100, Japan), scanning electron microscopy (SEM, FEI Quanta600, USA) and transmission electron microscopy (TEM, JEOL JEM-2100F, Japan) were used to evaluate the microstructure of the melted samples. Energy dispersive spectrometry (EDS) was used to analyze the chemical composition and impurity elements at specified positions from the surface to the inside of the ingots to establish the homogeneity. Phase identification of the compounds was performed by X-ray diffraction (XRD, D/max 2200PC, Japan) with Cu Kα radiation. The distribution of the species dissolved from the crucible into the melt was also determined by X-ray dot mapping. For the thermodynamic study of metal-crucible reactions, the overall oxygen and yttrium contents were measured by the inert gas infrared-thermal conductivity technique (IGI, LECO TC-436, USA) and inductively coupled plasma-atomic emission spectrometry technique (ICP-AES, P. E. Plasma 2000, USA), respectively. A HZX-1000 hardness tester with a load of 50 g for 15 s was used to measure the microhardness of the melted samples.

3. Results

3.1. Microstructure

Fig. 2 illustrates the EPMA micrographs of the cross-section of a Ti–47Al sample allowed to cool inside the crucible. As shown in Fig. 2a, the microstructure contained a fully lamellae constituent with two phases α_2 and γ phase at the sample surface. At higher distance from the surface, grains of γ phase appeared at the boundaries of lamellar grains (Fig. 2b), following the decrease in the cooling rate. Similarly, those samples poured into the graphite moulds also showed fully lamellae at the surface, and small grains of γ phase appeared at higher distance from the surface due to the low cooling rate.